Manuscript prepared for J. Name
with version 4.2 of the LaTeX class copernicus.cls.
Date: 4 October 2012

Impact of the Sea Surface Temperature forcing on hindcasts of Madden-Julian Oscillation events using the ECMWF model

Eric de Boisséson[1,2], **M. A. Balmaseda**[1], **F. Vitart**[1], **and K. Mogensen**[1]

[1]European Centre for Medium Range Forecast, Shinfield Park, RG2 9AX, Reading, UK
[2]CNRM/GAME, 42 avenue Gaspard Coriolis, 31057, Toulouse, France

Abstract. This paper explores the sensitivity of hindcasts of the Madden Julian Oscillation (MJO) to the use of different Sea Surface Temperture (SST) products as lower boundary conditions in the European Centre for Medium-range Weather Forecasts (ECMWF) atmospheric model. Three sets of monthly hindcasts experiments are conducted starting from initial conditions from the ERA interim reanalysis. First, as a reference, the atmosphere is forced by the SST used to produce ERA interim (ERAi SST). In the second and third experiments, the SST is switched to the OSTIA (Operational Sea Surface Temperature and Sea-Ice Analysis) and the AVHRR-only (Advanced Very High Resolution Radiometer) SST reanalyses, respectively. Tests on the temporal resolution of the SST show that monthly SSTs are not optimal while weekly and daily resolutions provide similar MJO scores. When using either OSTIA or AVHRR, the propagation of the MJO convection is degraded and the resulting MJO scores are lower than in the reference experiment. Further experiments show that this loss of skill cannot be attributed to either the difference in mean state or temporal variability between ERAi SST and both OSTIA and AVHRR products. Additional diagnostics show that the phase relationship between either OSTIA or AVHRR SST and the MJO convection is distorted with repspect to the observations and to the ERA interim reanalysis. This distortion impacting the MJO hindcasts leads to a relative loss of forecast skill. This result argues for the importance of a realistic representation of ocean-atmosphere interactions in MJO hindcasts and shows that not all SST products, even if accurate for other purposes, fullfill this requirement.

Correspondence to: Eric de Boisséson
(ne9@ecmwf.int)

1 Introduction

The Madden-Julian Oscillation (MJO) is the major mode of intraseasonal variability (ISV) in the tropical atmosphere (Zhang, 2005). It is characterized by an eastward propagation of regions of both enhanced and suppressed convection, mainly observed over the Indian and the Pacific Oceans. The MJO is known to influence the Asian (e.g., Murakami (1976), Yasunari (1979)) and Australian monsoon (Hendon and Liebmann , 1990), the evolution of El Nino events (e.g., Kessler and McPhaden (1995)) and the weather regimes over the North Atlantic European region in winter (Cassou , 2008; Vitart et al., 2010). The simulation and the predicatibility of such intraseasonal and seasonal weather regimes need an accurate representation of the MJO in General Circulation Models (GCM). While simulating the MJO used to be difficult in terms of propagation (Slingo et al., 1996) and of intensity of the ISV (Lin et al., 2006), new-generations models are now able to reproduce a correct MJO (Lin et al., 2008; Vitart et al., 2010). Because of its importance for the predictability at intraseasonal and seasonal time scales, the MJO is one of the main benchmarks for the skill of the extended-range forecast systems.

Air-sea interactions associated with the MJO are known to drive Sea Surface Temperature (SST) perturbations that may feedback to the atmospheric dynamics and influence the MJO signal (Hendon , 2005). Krishnamurti et al. (1998) observed from the FGGE (First GARP Global Experiment) data an instraseasonal signal of SST in the Indian and the western Pacific Oceans. This signal had a temporal phasing with surface westerly winds indicative of an ocean forced by the atmosphere. The air-sea flux and SST data provided by the 1.45°S-156°E mooring of the TOGA-COARE (Tropical Ocean Global Atmosphere Program's Coupled Ocean Atmosphere Response Experiment) program during the winter 1992-1993 (Anderson et al., 1998) clearly showed the response of SST to MJO surface fluxes. Warm SST anomalies

followed the suppressed phase of the MJO, while cold SST anomalies followed the convective phase of the MJO (Shinoda et al., 1998). Using satellite and reanalysis data, Woolnough et al. (2000) confirmed that the SST ISV is driven by the atmosphere via air-sea interactions.

The SST anomalies associated to the MJO are expected to influence the latent and sensible heat fluxes and thus affect the MJO signal. Both works from Woolnough et al. (2007) and Vitart et al. (2007) introduced ocean-atmosphere coupling in the Integrated Forecast System (IFS) of the European Center for Medium-range Weather Forecasts (ECMWF) in order to represent consistent MJO air-sea interactions. Woolnough et al. (2007) showed that ocean/atmosphere coupled predictions of the MJO were superior to predictions produced by persisting the inital SST conditions. Using the same coupled model, Vitart et al. (2007) showed that the MJO predictability is further increased when improving the parameterization of the atmospheric component, especially in terms of convection. These studies conclude that the simulation of the MJO needs an accurate representation of air-sea interactions through a good representation of the ISV and of the diurnal cycle of the SST.

Several studies have shown that the use of SST products with accurate ISV in atmosphere-only numerical models already improved the simulation of the MJO in terms variability, intensity and propagation. Reichler and Roads (2005) forced the National Centers for Environmental Prediction (NCEP) atmospheric model with weekly observed SST and reported an improvement of the MJO simulation compared to a model forced by a SST climatology. Kim et al. (2008) forced the Seoul National University atmospheric GCM with observed SST at monthly, weekly, and daily temporal resolutions. They showed that high temporal SST variability improved the simulation of the atmospheric ISV, the propagation of the MJO and increased the MJO forecast skill. Kim et al. (2010) also showed that the phase relationship between SST and MJO convection, even at daily temporal resolution, became distorted rapidly as the forecast lead time increased. The same phase relationship was maintained when using a coupled model, suggesting that coupling is needed to extend MJO predictability.

In recent years the increasing number of satellite instruments has enhanced the developement of SST analysis products, such as those from the Group for High-Resolution Sea Surface Temperature (GHRSST, see Donlon et al. (2007); http://www.ghrsst-pp.org/). While persistent clouds in the Tropics are problematic for satellite retrievals from infrared sensors, they are better handled by microwave sensors. However, microwave satellite observations from the Advanced Microwave Scanning Radiometer (AMSR, see http://www.ncdc.noaa.gov/) or the Tropical Rainfall Mesasuring Mission Microwave Imager (TMI, see http://www.ssmi.com/) are only avaible from the late 1990s and early 2000s. As our study needs SST reanalyses covering the early 1990s, it will only focus on products obtained using satellite observations from infrared sensors.

Among the GHRSST products that fullfil that requirement is the recent 1/4° daily OSTIA (Operational Sea Surface Temperature and Sea-Ice Analysis) SST reanalysis (Roberts-Jones et al., 2012) that spans the period January 1985-December 2007. This product uses both satellite retrievals from the Advanced Very High Resolution Radiometer (AVHRR) and the Along Track Scanning Radiometer (ATSR) and in-situ data. The 1/4° daily AVHRR-only reanalysis (Reynolds et al., 2007) also provides a consitent SST dataset from September 1981 onwards. As numerical weather prediction is one of the applications of such SST reanalyses, their potential impact on extended-range hindcast and atmospheric reanalysis activities has to be assessed. The ECMWF hindcasts and the ERA interim reanalysis (Dee et al., 2011) use SST from different sources according to the considered period: the 1x1° weekly NCEP 2d-var reanalysis from January 1981 to June 2001 (Reynolds et al., 2002), the 1x1° weekly NCEP OIv2 SST reanalysis from July 2001 to December 2001 (Reynolds et al., 2002), the daily 1/2° Real Time Global (RTG) SST analysis from January 2002 to January 2009 (Gemmill et al., 2007) and the 1/20° daily OSTIA from February 2009 onwards (Donlon et al., 2011). Before 1981 and the satellite era, the ECMWF reanalyses use the Hadley Centre Sea Ice and Sea Surface Temperature dataset (HADISST1) consisting of monthly SST and Sea Ice fields produced by the UK Met Office (Rayner et al., 2003).

This work is an attempt to assess the performance of the IFS in hindcasting winter MJO events when forced by different SST products at different temporal resolutions starting from the same ERA interim inital conditions. The winter 1992/1993 MJO is used as benchmark case at ECMWF as in Woolnough et al. (2007) and Vitart et al. (2007). As a reference, the IFS is forced with the observed SST used to produce ERA interim. Then the MJO forecast skill of the IFS is estimated when forced with the daily OSTIA and AVHRR-only SST reanalyses. The impact of the temporal resolution (daily, weekly, monthly) of the respective SST products is assessed by applying temporal running means to the SST fields. Then, the impact of changing the SST forcing fields from the reference (ERA interim SST) to the OSTIA and AVHRR-only reanalyses is investigated through the MJO forecast skill, the propagation of the MJO convection and the phase relationship between SST and the MJO convection. In the following, Section 2 will describe the SST products. Section 3 will focuse on the MJO experiments and their skill scores. Section 4 will investigate the phase relationship between SST and the MJO convection in the experiements. Section 5 will discuss the results and draw the conclusions of this study.

2 SST products

2.1 Description

For the 1992-1993 time period, ERA interim SST fields (referred to as ERAi SST) come from the NCEP 2Dvar SST, originally a weekly 1°x1° analysis (Reynolds et al., 2002) available from 1981. This analysis combines the information from in situ data (from ships and buoy) from the Comprehensive Ocean-Atmosphere Data Set (COADS before 1998) and the Global Telecommunication System (GTS after 1998) and from the AVHRR satellite. In situ data provide a large-scale bias correction of the satellite data. The bias correction is done using a preliminary 2Dvar analysis of the difference between weekly satellite data and in situ data on a 1°grid (Reynolds et al., 2002). In situ data and corrected satellite observations are then analysed using a 2Dvar procedure. Weekly SSTs were then daily linearly interpolated for the building of ERA interim (Fiorino , 2004). The ERAi SST are consistent with the initial atmospheric conditions of the MJO experiments. Compared to the version 2 of the Optimal Interpolation procedure (OIv2, Reynolds et al. (2002)), the 2Dvar is known to have a too large correlation scale (1650 km) in the bias correction step and to produce somewhat smoother SST fields and smaller meridional gradients in the equatorial Pacific (Fiorino , 2004).

The daily 1/4° AVHRR-only reanalysis (Reynolds et al., 2007) uses similar data as the 2D-var SST but more up to date (ICOADS dataset and AVHRR satellite). All data are used for a given day and the SST are analysed using the OIv2 procedure. OIv2 includes a temporal smoothing within the 3-day assimilation window where the middle day (the day of the analysis) is weigthed higher than the other two days. The error correlation scales range from 50 to 200 km according to geographical region. The diurnal cycle of SST is ignored in the analysis. However, as the OI analysis is a daily average SST that is bias adjusted using a spatially smoothed 7-day in situ SST average, the impact of the dirunal cycle is reduced.

The daily 1/4° OSTIA reanalysis (Roberts-Jones et al., 2012) combines the information from the ICOADS in situ dataset, the Ocean Sea Ice Satellite Application Facility (OSI SAF) sea ice concentration data, the AVHRR satellite and the ATSR instruments on board of the ERS-1, ERS-2 and ENVISAT satellites. The SST is analysed using a multiscale OI-type scheme in a 72h window centered on 1200 UTC on the analysis day (see Roberts-Jones et al. (2012) for more details). Higher weight is given to observations closest to the analysis day. Two error correlation scales - 10 and 100 km - are used depending on the region and the input data. The OSTIA product provides an estimate of the foundation SST as defined by the GHRSST, i.e. a SST free of diurnal warming.

2.2 General comparison

The main differences between OSTIA/AVHRR and ERAi SST come from their repective mean state and the additional noise associated to their daily frequency. On average over the winter 1992-1993, the OSTIA SST are overall colder than ERAi SST by 0.18°C in the Tropics. Apart from some warmer patches, OSTIA SST are particularly colder (sometimes by more than 0.4°C) in the western part of the Maritime Continent, in the Pacific cold tongue and in the Tropical Atlantic (Fig.2a). AVHRR SST are also overall colder than ERAi SST in the Tropics particularly in the western Indian Ocean (from 0.2 to 0.8°C colder) over the Maritime Continent and in the western Pacific (Fig.2b). Over the winter 1992-1993, the OSTIA and AVHRR daily products show much more variability than the ERAi SST (only daily interpolated from a weekly product) all over the Tropical area (Fig.3). OSTIA and AVHRR are overall similar. The AVHRR reanalysis shows slightly more variability than OSTIA in the eastern Indian Ocean, the western and central Pacific and the tropical Atlantic Oceans and slightly less in the western Indian Ocean and eastern Pacific Ocean (Fig.3a,b).

At the TAO station 2°S-156°E, the OSTIA and AVHRR products seem overall closer to in situ observations than ERAi SST over the winter 1992-1993 (Fig.4). As expected, OSTIA and AVHRR SST show more variance than ERAi SST (0.16 and 0.17 versus 0.9), which matches the observations (variance of 0.17). Among the three SST products, OSTIA shows the best correlation with the observations (0.9). AVHRR and ERAI have similar correlations (0.75). The relatively low correlation of AVHRR SST is due to large variability signals characterized by extrema of SST that are not found in the other products. These extrema also lead to a relatively high root mean square error (0.32 versus 0.21 for OSTIA and 0.27 for ERAi). These time series show that the atmosphere of the MJO hindcasts will see quite different boundary conditions according to the chosen forcing set.

In the context of the MJO hindcasts, the SST fields from AVHRR-only and OSTIA reanalyses are interpolated on the spectral grid of the atmospheric model T_L159 (1.125x1.125 at the Equator) with an inverse-distance-weighted interpolation scheme using the information of the 8 closest grid points. The interpolation smoothes the spatial variability of the AVHRR and OSTIA fields, but the resulting SST are never as smooth as ERAi SST.

3 MJO experiments

3.1 Experiment settings

The experimental settings of the MJO hindcasts are similar to the ones described in Woolnough et al. (2007) and Vitart et al. (2007). Briefly, each experiment consists of a series of 32-day forecasts using a five-member ensemble initialized

at 0000 UTC each day from 15 December 1992 to 31 January 1993. In our experiments, the atmospheric component is the ECMWF IFS cycle 36R4. The horizontal resolution is T_L159 with 62 vertical levels. The atmospheric initial conditions come from the ERA interim reanalysis (Dee et al., 2011). A skin layer scheme has been implemented in the IFS to simulate the diurnal variations of SST (see Zeng and Beljaars (2005) and Takaya et al. (2010)).

For comparative purposes in the discussion, a coupled ocean-atmosphere version of the IFS is used. The atmospheric component is the same as in atmosphere-only mode. The oceanic component is the NEMO (Nucleus for European Modelling of the Ocean, Madec (2008)) ocean GCM (OGCM) version 3.0 with 42 vertical levels, a resolution in the extratropics of about 1° and a higher meridional resolution in the equatorial region (about 0.3°). This coupled model is used in the ECMWF seasonal forecast system and more details are given in Molteni et al. (2011).

In the main part of the study, three sets of MJO experiments (see Table 1) are conducted in atmosphere-only mode. First, as a reference experiment, the atmosphere is forced by ERAi SST that are daily interpolated from a weekly reanalysis (see Section 2.1). An additional experiment uses ERAi SST at a monthly resolution. The second set uses the OSTIA SST reanalysis at daily, weekly and monthly resolutions. To assess the impact of the difference of mean state between OSTIA and ERAi, an additional experiment is run where the mean state of OSTIA SST is corrected in each forecast by removing the averaged difference between OSTIA SST and ERAi SST over the forecast length. The third set of experiments uses the AVHRR-only SST reanalysis at daily, weekly and monthly resolutions. As for the OSTIA product, the experiment with correction of the mean state with respect to ERAi SST is also run. The transition from daily to weekly and from daily to monthly resolution is performed by applying a running mean on the original SST fields centered on the day of the corresponding forecast lead time.

3.2 Diagnostic procedure

The skill of prediction of the MJO is evaluated according to the method described in Wheeler & Hendon (2004). This method considers that the intraseasonal variability of the MJO can be captured by a combined Empirical Orthogonal Function (EOF) analysis of the anomalies (with respect to the 1991-2003 climate) of the zonal wind at 200-hPa and 850-hPa and of the Outgoing Longwave Radiation (OLR) averaged between 10°S and 10°N. Wheeler & Hendon (2004) showed that most of the MJO variability is described by the two first components of the combined EOF analysis. Their longitudinal patterns can represent all the active and suppressed phases of the MJO (Fig.1) over its eastward propagation. Negative OLR extrema reflect the position of the convective centre of the MJO. According to the sign of the associated Principal Component (PC), the convective centre on EOF1 is located over the Maritime Continent ($PC1 > 0$) or over the Western Hemisphere and Africa ($PC1 < 0$). On EOF2, the convection is over the Pacific Ocean ($PC2 > 0$) or over the Indian Ocean ($PC2 < 0$). The recommended score of the MJO forecast relies on the correlation of the monthly ensemble-mean forecasts with the two first PCs of the combined EOFs estimated from the ERA interim atmospheric reanalysis. The method for computing the MJO scores of this study is detailed in Vitart et al. (2007). According to Woolnough et al. (2007), two MJO events occur between mid-December 1992 and February 1993. The 47 starting dates of the experiments include all the phases of these MJO events as identified by the combined EOF analysis. Plus, each forecast captures each phase of the MJO at least once.

3.3 Scores

The impact of the temporal resolution of the SST forcing on the forecast skill is first addressed by comparing the MJO hindcasts performed with daily, weekly amd monthly SST fields from the OSTIA and AVHRR-only reanalyses. Concerning the OSTIA product, the correlations of the ensemble-mean forecast with the two principal components of the combined EOF are similar for the three temporal resolution until day 6 of the forecast (Fig.5a). The daily and weekly experiments show similar scores on PC1 and 2. The skill is higher than 0.8 up to days 17 and 19 on PC1 and 2 and remains significant (correlations higher than 0.6) until days 22 and 23, repectively. With respect to higher resolution experiments, the monthly experiment shows a loss of skill of at least 2 days from day 10 throughout the forecast lead time on PC1. On PC2, the monthly experiment maintains a good skill until day 13 that rapidly decays to ultimately show a loss of 6 days of significant skill.

The monthly experiment using the AVHRR product show very similar skill as its OSTIA equivalent but the gap between the monthly and weekly-daily resolution is reduced with a loss of signifiant skill of 1 to 2 days on PC1 and 2 to 3 days on PC2. As for OSTIA, the daily and weekly experiments show similar scores (Fig.5b). The scores of the weekly experiment looks a bit better especially on PC1 with a gain of significant skill of 1 day at day 22 with respect to the daily experiment. On PC2, both experiment shows significant skill until day 20. Differences between weekly and daily experiments nevertheless remains within the forecast spread.

At full temporal resolution, the scores of the OSTIA product are better than for AVHRR especially on PC2 where the OSTIA experiment shows a gain of skill of 3 days (Fig.5c). But the MJO scores obtained when using these two SST products remains lower than when using ERAi SST. Both OSTIA and AVHRR experiments show a loss of significant skill of 2 days on PC1 and much more on PC2 where the predictability when using ERAi SST stays high throughout the forecast with correlations hgher than 0.7. As an indication, OSTIA and AVHRR forcings still produce much bet-

ter MJO than when the resolution of ERAi SST is reduced to monthly which give similar scores as monthly OSTIA or AVHRR fields.

Another interesting point is that weely and daily forced experiments produce similar scores showing that the additional noise associated to the daily variability of the OSTIA and AVHRR-only reanalyses is not the reason why forcing the atmosphere with these two products does not provide as good results as when using ERAi SST that derived from weekly fields (Fig.5a,b). Similarly, there is no improvement of the MJO scores when correcting the mean state of the OSTIA and AVHRR-only products with respect to ERAi SST in the MJO hindcast. The differences in MJO skills thus do not directly come from these obvious differences in the SST products.

3.4 MJO signal

To visualise how the experiments forced by the three SST products differ, the propagation of the MJO signal in the forecasts is tracked in longitudinal hovmoller diagrams of ensemble-mean OLR anomalies averaged between 10°S and 10°N. In Fig.6, the forecasts and their equivalent in the ERA interim analysis are averaged for starting dates when the convective centre of the MJO is over the Indian Ocean. In the analysis (Fig.6a), the MJO convective centre (negative OLR anomalies) propagates from the Indian to the central Pacific Ocean and is followed by a phase of suppressed convection (positive OLR anomalies) a few days later. The ERAi experiment simulates correctly this propagation but the MJO active and suppressed phases are much weaker than in the analysis (Fig.6b). The weakening is particarly marked when the convection reaches the Maritime Contient that is know as a barrier for the MJO simulation (Inness et al., 2003). In the OSTIA experiment, the MJO convective signal is even weaker over the Maritime Continent and its eastern propagation is hardly visible (Fig.6c). There is no visible propagation of the suppressed phase that is stuck over the Maritime Continent. In the AVHRR experiment, the propagation of the convective phase of the MJO is slightly more pronounced but a signal of suppressed convection remains over the Indian Ocean throughout the rest of the forecast without any sign of the following convective signal that appears in the ERA interim reanalysis (Fig.6d).

4 Phase relationship between SST forcing and MJO convection

The only difference between the experiments is the SST fields that the atmosphere receives as lower boundary conditions. Kim et al. (2008) and Kim et al. (2010) showed that, in the observations, the suppressed MJO convection leads enhanced SST and that active MJO convection follows enhaced SST after several days. They also show that, according to the SST that the atmosphere sees, this relationship becomes more or less distorted with increased lead time leading to the degradation of the MJO hindcasts over the winters 1998-2004. One can thus expect to see the differences in the scores of the MJO experiments described in Section 3.3 being reflected by obvious differences in the corresponding SST-convection phase relationship.

4.1 Phase relationship between SST and convection: observations

The SST-convection phase relationship is estimated in the Indian Ocean over the winters (December-February) 1985-2006 chosen as the common winter period for ERAi, OSTIA and AVHRR SST products. The observed OLR (indicative of the convection) comes from the National Oceanic and Atmospheric Administration (NOAA) daily interpolated OLR (see Liebmann and Smith (1996)). The NOAA interpolated OLR is produced from the NOAA satellite retrievals on a 2.5°x2.5° grid and is available from 1979 onwards. The phase relationship between SST and convection is produced from filtered SST and OLR anomalies with respect to their respective 1985-2006 mean averaged in the Indian Ocean box 5°S-5°N,60°-95°E. Following the method of Kim et al. (2008), for each date, the interannual variability of SST and OLR is removed by substracting their respective 32-day mean (the 32 days following the considered date). The intraseasonal variability is then extracted from SST and OLR by applying a 5-day running mean. When using ERAi SST and NOAA OLR, the lag-correlation between SST and OLR shows a near-quadrature phase relationship (Fig.7): positive OLR anomalies (suppressed convection) lead enhanced SST, and negative OLR (enhanced convection) lag enhanced SST after several days. The extremum correlations occur at lag -10 days (0.45) and +12 days (-0.38). The phase relationship in ERA interim is similar in shape but with slightly smaller amplitude: 0.39 and -0.37. When using OSTIA SST with either NOAA or ERA interim OLR, the phase relationship still has a quasi-quadrature shape but the extremum correlations are shifted by almost 3 days toward the negative lags. The amplitude of the relationship is also weaker than in ERA interim (extremum correlations around 0.27 and -0.21). The OSTIA reanalysis thus provides a relatively weak relationship between SST and the current atmospheric products on intraseasonal time-scale. When using AVHRR SST, the phase relationship is not quadratic anymore. The maximum correlation (0.3) coincides with the 0 lag and the minimum correlation (-0.33) only happens at lag +17 days. The AVHRR-only reanalysis is thus off the expected phase relationship between ocean and MJO convection in the Indian Ocean.

4.2 Phase relationship between SST and convection: MJO experiments

To investigate the relationship between SST and convection as simulated in the MJO hindcasts, additional experiments are conducted over the winters 1985-2006. These expiments include 5 forecasts per winter, every 15 days from the 1st December to the 1st February. The configuration is the same as for previous experiments (see Section 2.1). The atmosphere is forced by the OSTIA and AVHRR-only reanalyses and by the ERAi SST. As mentioned in the Introduction, over 1985-2006, ERAi SST are produced from the 1x1° weekly NCEP 2Dvar reanalysis from January 1981 to June 2001, the 1x1° weekly NCEP OIv2 SST reanalysis from July 2001 to December 2001 and the daily 1/2° RTG SST analysis from January 2002. For comparative purposes, a similar experiment is conducted in coupled mode and its results are discussed in the next and final section.

These 22-winter experiments provide enough data to investigate the phase relationship between the SST forcing and the simulated atmospheric convection (OLR) according to the forecast lead time. This relationship is estimated in a similar way as in Section 4.1. The interannual variability in each 32-day forecast is removed by substracting its 32-day mean. The intraseasonal variability is then extracted by applying a 5-day running mean in each forecast segment. The evolution of the phase relationship between SST and OLR in the Indian Ocean (5°S-5°N,60°-95°E) according to the lead time in the three forced experiments is compared to its equivalent in the ERA interim analysis. As seen in Section 4.1 (Fig.7), the analysis show a near-quadrature phase relationship (Fig.8). Extremum correlations occur around 7-10 days according to the considered forecast week. Forcing with either OSTIA SST or ERAi SST produce similar phase relationships that are, though sometimes weakened, overall close to the analysis until week 3 of the forecast. The forecast forced by OSTIA is nevertheless slightly shifted toward negative lags in week 1 of the forecast. The phase relationship is recovered in week 2 and 3 but with lower correlations than in the ERAi experiment when the lag is negative in week 2 and 3. The OSTIA experiment loses the quadrature phase relationship in week 4 of the forecast while the ERAi experiment keeps some consistency with the analysis. When forcing with AVHRR SST, there is no quadrature phase relationship between SST and convection in week 1. The shape of the phase relationship is more consitent with the observed one (Fig.7). In weeks 2 and 3, the quadrature shape is recovered but the correlation are very weak and the timing do not match the analysis at all. In week 4, as in the OSTIA experiment, the quadrature is lost again.

The experiments using either OSTIA or AVHRR SST have something in common: their phase-relationship is distorted in the first days of the forecast before the quadrature is more or less recovered in the following days. This suggests that the atmosphere initialized using ERAi SST needs some time to adapt to a different set of lower boundary conditions. This situation is not ideal in the perspective of predicting a MJO events as a degraded phase relationship between SST and convection implies less efficiency to maintain and propagate the MJO signal (Kim et al., 2008). This is reflected on the scores of these 22-winter experiments that show lower forecast skill when using either OSTIA or AVHRR SST than when using ERAi SST (Fig.9).

5 Discussion an conclusion

SST analyses are an important component of numerical weather prediction system. They are used to force atmospheric model in hindcast and reanalysis acticvities that are crucial for the improvement of the short and extended range weather forecasts. This study mainly explores the sensitivity of hindcasts of the MJO to a change of SST boundary conditions from ERAi SST to either OSTIA or AVHRR-only SST reanalyses. On the other hand, the sensitivity of the scores of the MJO hindcasts to the temporal resolution of the different SST products is also assessed. The study mainly focuses on the winter MJO of 1992-1993 used as a benchmark case for the ECMWF monthly forecasting system (Vitart et al., 2007).

Whatever the considered product, a SST with monthly temporal resolution is not optimal for hindcasting the 1992-1993 MJO. The resulting scores show a relative loss of at least 2 days of significant skill compared to a daily or weekly SST product (Fig.5a,b). This is consistent with results from Kim et al. (2008) and Klingaman et al. (2008) who showed a relative loss of predictability in the Tropics when forcing the atmosphere with a monthly SST product. Daily and weekly SST products however show similar forecast skills. When switching from ERAi SST to either OSTIA or AVHRR SST, the skill of the 1992-1993 MJO hindcast is relatively degraded. Additional experiment show that the differences between these two SST products and the ERAi SST in terms of temporal variability and mean state (see Figs.3 and 2) are not the main reasons for this degradation.

Instead, this study suggests that the relative loss of skill comes from a distortion of the phase relationship between the SST and the MJO convection when switching from ERAi SST to either OSTIA or AVHRR SST. Computing this phase relationship from ERAi SST and observed OLR provides the quadrature phase-relationship between ocean and atmosphere on intraseasonal timescales already reported in other studies (Zheng, 2004; Rajendran and Kitoh , 2006; Kim et al., 2008; Maloney et al., 2008; Saha et al., 2010; Kim et al., 2010). The same diagnostic with either OSTIA or AVHRR SST shows a relatively distorted relationship (Fig.7) that is visible in the first days of the MJO hindcasts forced by either of these SST products (Fig.8). The forecast lead time increasing, the atmosphere seems to adapt to the SST fields to recover the expected quadrature. This pattern most probably reflects the initialization shock following the switch from

ERAi SST, used to initialize the model, to OSTIA or AVHRR SST boundary conditions.

Difference of spatial patterns between SST products can be an additional source of loss of MJO forecast skill. Even smoothed by the interpolation from their original grid to the atmospheric one, the resulting SST fields are not as smooth as ERAi SST. Switching to noisier lower boundary conditions may generate air-sea interactions weakening the MJO signal in a low resolution atmosphere starting from an initial state produced using smooth ERAi SST. The Maritime Continent being a barrier to the MJO prediction, an initially weakened MJO signal will have difficulties to propagate over and past this barrier as described on Fig.6. A way to assess the impact of the switch of boundary conditions would be to produce an atmospheric reanalysis with either OSTIA or AVHRR SST forcing and perform again the MJO hindcasts using the new inital conditions.

Several studies (Zheng, 2004; Rajendran and Kitoh , 2006; Kim et al., 2008; Maloney et al., 2008; Saha et al., 2010; Kim et al., 2010) show that the ocean-atmosphere coupling improves the phase relationship between SST and convection (or precipitation) at intraseasonal timescale. For comparative purposes, similar MJO hindcasts are performed in coupled mode over the winter 1985-2006. The coupled experiment provides an intense quadrature phase relationship between SST and convection up to week 3 of the hindcasts (Fig.8). The coupling provides a tighter (higher correlations) ocean-atmosphere connection than in atmosphere-only mode and, more surprisingly, than in the analysis or the observations (Figs.7 and 8). The scores of the 22-winters MJO hindcasts for the coupled experiment show a significant gain of skill compared to the forced experiment on PC2 (Fig.9), when the MJO active centre interacts more frequently with the ocean (see Section 3.2). The persistence of the skill on PC2 is consistent with the maintenance of a strong SST-convection phase relationship throughout the hindcasts. The extent to which the relative gain of MJO skill in the coupled experiment is linked to a phase relationship substantiallly stronger than the observed one and wether this is realistic or not need to be investigated in future works.

To conclude, this study shows that switching to SST boundary conditions that are different from the inital conditions has a negative impact on the skill of MJO hincasts. The phase relationship diagnostic gives insights on how ocean-atmosphere coupled processes are perturbed by this switch. This diagnostic highlights how important realistic ocean-atmosphere interactions are in MJO hindcasts. This conclusion is reinforced when assessing the impact of a coupled system on such hindcasts. This study is however far from being exhaustive. For example, such MJO experiments could be repeated with other versions of the ECMWF model, other atmospheric models, at higher resolution, and over other periods and could focus on other event than the 1992-1993 winter MJO. Using more recent periods would also allow to test the impact AMSR and TMI SST products derived from microwave sensor measurements in the Tropics where persistent coulds disturb infrared satellite retrievals. A last interesting point would be to assess the impact of a sub-daily SST forcing on the atmosphere and to compare it to a coupled system.

Acknowledgements. Eric de Boisseson is supported by CNRS-INSU and ECMWF. This is a contribution to the MyOcean project.

References

Anderson, S. P., R. A. Weller, R. B. Lukas, 1996. Surface buoyancy forcing and the mixed layer of the western Pacific warm pool: observations and 1D model results. J. Climate, 9: 30563085, doi: http://dx.doi.org/10.1175/1520-0442(1996)009

Cassou C., 2008, Intraseasonal interaction between the MaddenJulian Oscillation and the North Atlantic Oscillation, Nature, 455, 523-527

Dee D. P., S. M. Uppala, A. J. Simmons, P. Berrisford, P. Poli, S. Kobayashi, U. Andrae, M. A. Balmaseda, G. Balsamo, P. Bauer, P. Bechtold, A. C. M. Beljaars, L. van de Berg, J. Bidlot, N. Bormann, C. Delsol, R. Dragani, M. Fuentes, A. J. Geer, L. Haimberger, S. B. Healy, H. Hersbach, E. V. Holm, L. Isaksen, P. Kallberg, M. Kohler, M. Matricardi, A. P. McNally, B. M. Monge-Sanz, J.-J. Morcrette, B.-K. Park, C. Peubey, P. de Rosnay, C. Tavolato, J.-N. Thepaut and F. Vitart, 2011, The ERA-Interim reanalysis: configuration and performance of the data assimilation system, Q. J. R. Meteorol. Soc. 137: 553597, April 2011 A

Donlon, C., I. Robinson, K. Casey, J. Vasquez, E. Armstrong, C. Gentemann, D. May, P. LeBorgne, J. Pioll, I. Barton, H. Beggs, D. J. S. Poulter, C. Merchant, A. Bingham, S. Heinz, A. Harris, G. Wick, B. Emery, A Stuart-Menteth, P. Minnett, B. Evans, D. Llewellyn-Jones, C. Mutlow, R. Reynolds, H. Kawamura and N. Rayner, 2007: The Global Ocean Data Assimilation Experiment High-resolution Sea Surface Temperature Pilot. Bull. Amer. Meteor. Soc., 88, 11971213

Donlon, C. J., M. Martin, J. D. Stark, J. Roberts-Jones, E. Fiedler and W. Wimmer, 2011. The Operational Sea Surface Temperature and Sea Ice analysis(OSTIA). Remote Sensing of the Environment. doi: 10.1016/j.rse.2010.10.017 2011

Fiorino, M., 2004. A multi-decadal daily sea surface temperature and sea ice concetration data set for the ERA-40 reanalysis. ERA-40 Project Report Series No 12, ECMWF: Reading, UK

Gemmill W, B. Katz, X. Li, 2007, Daily, Real-Time, Global Sea Surface Temperature - High Resolution Analysis: RTG SST HR. NCEP/EMC Office Note, pp. 39

Hendon H. H., and B. Liebmann, 1990: A composite study of onset of the Australian summer monsoon. J. Atmos. Sci., 47, 22272240

Hendon H. H., 2005. Air-sea interaction. In: Intraseasonal Variability in the Atmosphere-Ocean Climate System, Lau W. K. M., Waliser D. E., (eds.), Springer Praxis Books, 223-246

Inness P. M, J. M. Slingo, E. Guilyardi and J. Cole, 2003, Simulation of the MaddenJulian Oscillation in a Coupled General Circulation Model. Part II: The role of the basic state. J. Climate, 16, 365382

Kessler, K. S., and M. McPhaden, 1995: Oceanic equatorial waves and the 199193 El Nio. J. Climate, 8, 17571774

Kim H. M., Hoyos C. D., Webster P. J., Kang I. S., 2008, Sensitivity of MJO Simulation and Predictability to Sea Surface Temperature Variability. J. Climate, 21, pp. 5304-5317

Kim H. M., Hoyos C. D., Webster P. J., Kang I. S., 2010, Ocean-atmosphere coupling and the boreal winter MJO. Clim. Dyn., 35: 771-784, doi 10.1007/s00382-009-0612-x

Klingaman N. P., Woolnough S. J., Weller H., Slingo J. M., 2008, The Importance of High-Frequency Sea Surface Temperature Variability to the Intraseasonal Oscillation of Indian Monsoon Rainfall, J. Climate, 21 (23), pp. 6119-6140, doi: http://dx.doi.org/10.1175/2008JCLI2329.1

Krishnamurti, T. N., D. K. Oosterhof, and A. V. Metha, 1988. Air-sea interaction on the timescale of 3050 days. J. Atmos. Sci., 45, 13041322

Liebmann B. and C.A. Smith, 1996: Description of a Complete (Interpolated) Outgoing Longwave Radiation Dataset. Bull. Amer. Meteor. Soc., 77, 1275-1277

Lin J. L., Kiladis G. N., Mapes B. E., Weickmann K. M., Sperber K. R., Lin W., Wheeler M., Schubert S. D., Del Genio A., Donner L. J., Emori S., Gueremy J-F., Hourdain F., Rasch P. J., Roeckner E., Scinocca J.F., 2006. Tropical Intraseasonal Variability in 14 IPCC AR4 Climate Models Part I: Convective Signals. J. Climate 19: 26652690

Lin,.H., G. Brunet, and J. Derome (2007): Intraseasonal variability in a dry atmospheric model. J. Atmos. Sci., 28, 702-708

Lin, H., G. Brunet, and J. Derome, 2008: Forecast skill of the Madden-Julian Oscillation in two Canadian atmospheric models. Mon. Wea. Rev., 136, 4130-4149

Madec, G., 2008, NEMO ocean engine, Tech. Rep. 27, Notes du pôle de Modélisation - Institut Pierre-Simon Laplace, 300pp.

Maloney, E. D., D. B. Chelton, S. K. Esbensen, 2008. Subseasonal SST Variability in the Tropical Eastern North Pacific during Boreal Summer. J. Climate, 21: pp. 4149-4167, doi: http://dx.doi.org/10.1175/2007JCLI1856.1

K. S. Mogensen, M. A. Balmaseda and A. Weaver: The NEMOVAR ocean data assimilation as implemented in the ECMWF ocean analysis for system 4. ECMWF Technical Memorandum No. 668, February 2012

Molteni, F., T. Stockdale, M. Balmaseda, G. Balsamo, R. Buizza, L. Ferranti, L. Magnusson, K. Mogensen, T. Palmer and F. Vitart, 2001. The new ECMWF seasonal forecast system (Sytem 4). ECMWF Tech. Memo. No 656, November 2011.

Murakami T., 1976: Cloudiness fluctuations during the summer monsoon. J. Meteor. Soc. Japan, 54, 175181

Rajendran, K. and A. Kitoh, 2006. Modulation of Tropical Intraseasonal Oscillations by OceanAtmosphere Coupling. J. Climate, 19: 366-391 doi: http://dx.doi.org/10.1175/JCLI3638.1

Rayner, N. A.; Parker, D. E.; Horton, E. B.; Folland, C. K.; Alexander, L. V.; Rowell, D. P.; Kent, E. C.; Kaplan, A. (2003) Global analyses of sea surface temperature, sea ice, and night marine air temperature since the late nineteenth century, J. Geophys. Res., Vol. 108, No. D14, 4407 10.1029/2002JD002670

Reichler, T. and J. O. Roads, 2005. Long-range predictability in the tropics. part II: 3060-day variability. J. Climate, 18: 634650, doi: http://dx.doi.org/10.1175/JCLI-3295.1

Reynolds R. W., N. A. Rayner, T. M. Smith, D. C. Stokes and W. Wang, 2002, An Improved In Situ and Satellite SST Analysis for Climate. J. Climate, 15: 16091625.

Reynolds R. W., T. M. Smith, C. Liu, D. B. Chelton, K. S. Casey, M. G. Schlax, 2007, Daily High-Resolution-Blended Analyses for Sea Surface Temperature. J. Climate, 20: 5473-5496, doi: http://dx.doi.org/10.1175/2007JCLI1824.1

Roberts-Jones J., E. K. Fiedler and M. J. Martin, 2012, Daily, Global, High-Resolution SST and Sea Ice Reanalysis for 1985-2007 Using the OSTIA System. J. Climate, 25: 6215-6232, doi: 10.1175/JCLI-D-11-00648.1

Saha, S., and Coauthors, 2010: The NCEP climate forecast system reanalysis. Bull. Amer. Meteor. Soc., 91, 10151057, doi: http://dx.doi.org/10.1175/2010BAMS3001.1

Shinoda, T., H. H. Hendon and J. Glick, 1998. Intraseasonal variability of surface fluxes and sea surface temperature in the tropical western Pacific and Indian oceans. J. Climate, 11: 16851702, doi: http://dx.doi.org/10.1175/1520-0442(1998)011

Slingo J. M., Sperber K. R., Boyle J. S., Ceron J-P., Dix M., Dugas B., Ebisuzaki W., Fyfe J., Gregory D., Gueremy J-F., Hack J., Harzallah A., Inness P., Kitoh A., Lau WK-M., McAvnaey B., Madden R., Matthews A., Palmer T. N., Park C-K., Randall D., Renno N., 1996. Intraseasonal oscillations in 15 atmospheric general circulation models: Results from an AMIP diagnostic subproject. Climate Dyn. 12: 325357

Takaya Y., J.-R. Bidlot, A. C. M. Beljaars, P. A. E. M. Janssen, 2010, Refinements to a prognostic scheme of skin sea surface temperature, J. Geophys. Res., 115, C06009, doi:10.1029/2009JC005985

Vitart F., S. J. Woolnough, M. A. Balmaseda, A. M. Tompkins, 2007, Monthly Forecast of the MaddenJulian Oscillation Using a Coupled GCM, Monthly Weather Review, 135, 2700-2715

Vitart F., F.Molteni, 2010, Simulation of the MaddenJulian Oscillation and its teleconnections in the ECMWF forecast system, Q. J. R. Meteorol. Soc. 136: 842855, April 2010 B

Wheeler M. C., H. H. Hendon, 2004, An All-Season Real-Time Multivariate MJO Index: Development of an Index for Monitoring and Prediction, Monthly Weather Review, 132, 1917-1932

Woolnough, S. J., J. M. Slingo and B. J., Hoskins, 2000. The Relationship between Convection and Sea Surface Temperature on Intraseasonal Timescales. J. Climate, 13: pp. 2086-2104, doi: http://dx.doi.org/10.1175/1520-0442(2000)013

Woolnough S. J., F. Vitart, M. A. Balmaseda, 2007, The role of the ocean in the MaddenJulian Oscillation: Implications for MJO prediction, Q. J. R. Meteorol. Soc. 133: 117128

Yasunari T., 1979: Cloudiness fluctuations associated with the Northern Hemisphere summer monsoon. J. Meteor. Soc. Japan, 57, 225242

Zeng X., and A. Beljaars 2005, A prognostic scheme of sea surface skin temperature for modeling and data assimilation. Geophys. Res. Lett., 32, L14605

Zhang C., 2005, Madden-Julian Oscillation, Rev. Geophys., 43, RG2003, doi:10.1029/2004RG000158

Zheng Y., D. E. Waliser, W. F. Stern and C. Jones, 2004. The Role of Coupled Sea Surface Temperatures in the Simulation of the Tropical Intraseasonal Oscillation. J. Climate, 17: pp. 4109-4134, doi: http://dx.doi.org/10.1175/JCLI3202.1

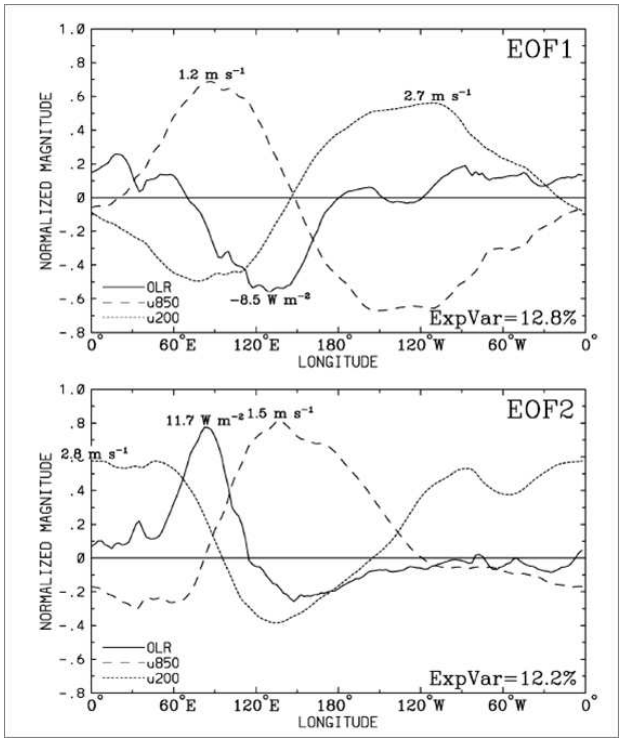

Fig. 1. Fig.1 from Wheeler & Hendon (2004). Spatial structures of EOFs 1 and 2 of the combined analysis of anomalies of OLR, and of zonal wind (u) at 850, and 200hPa. The variance explained by the respective EOFs is 12.8% and 12.2%..

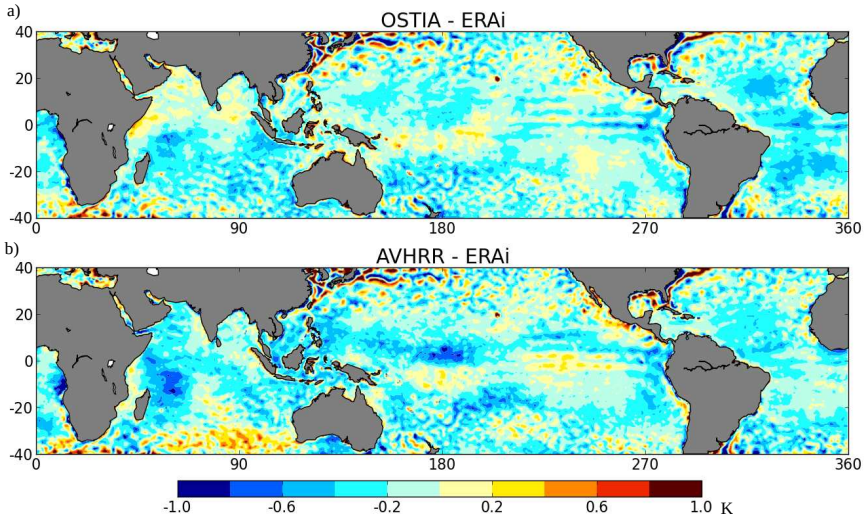

Fig. 2. a) Difference between OSTIA and ERAi SST (in K) averaged over the winter (December to March) 1992-1993 in the Tropics. b) Same as a) for AVHRR SST.

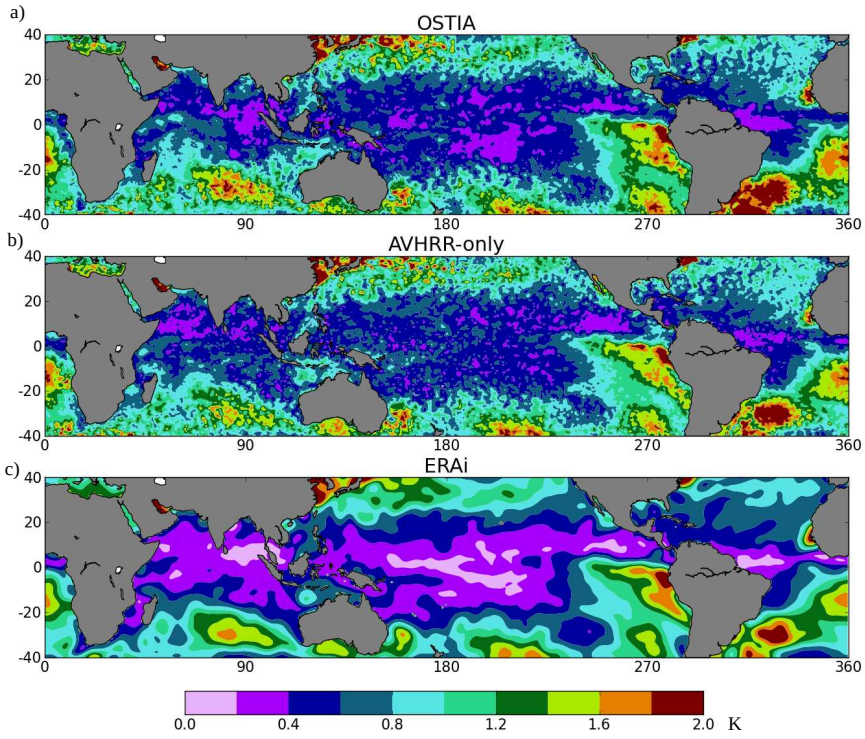

Fig. 3. a) Standard deviation (in K) of OSTIA SST over the winter (December to March) 1992-1993 in the Tropics. b) and c) Same as a) for AVHRR SST and ERAi SST, respectively.

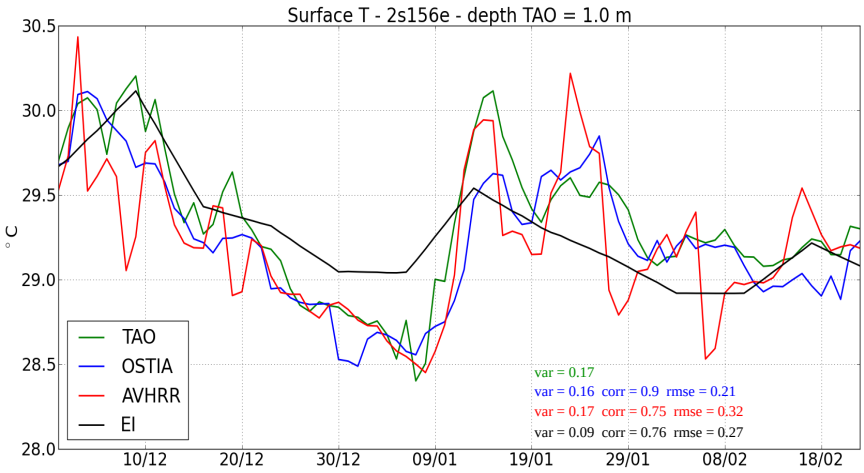

Fig. 4. In situ SST (temperature observed at 1 m depth, TAO, green line), OSTIA SST (OSTIA, blue line), AVHRR SST (AVHRR, red line) ERAi SST (EI, black line) at the TAO station 2°S-156°E from December 1992 to March 1993. SST in °C. On the background is written the variance (var) associated to each SST product. For the OSTIA, AVHRR and ERAi SST, the correlation (corr) and the root mean square error (rmse) with respect to the TAO SST are also provided.

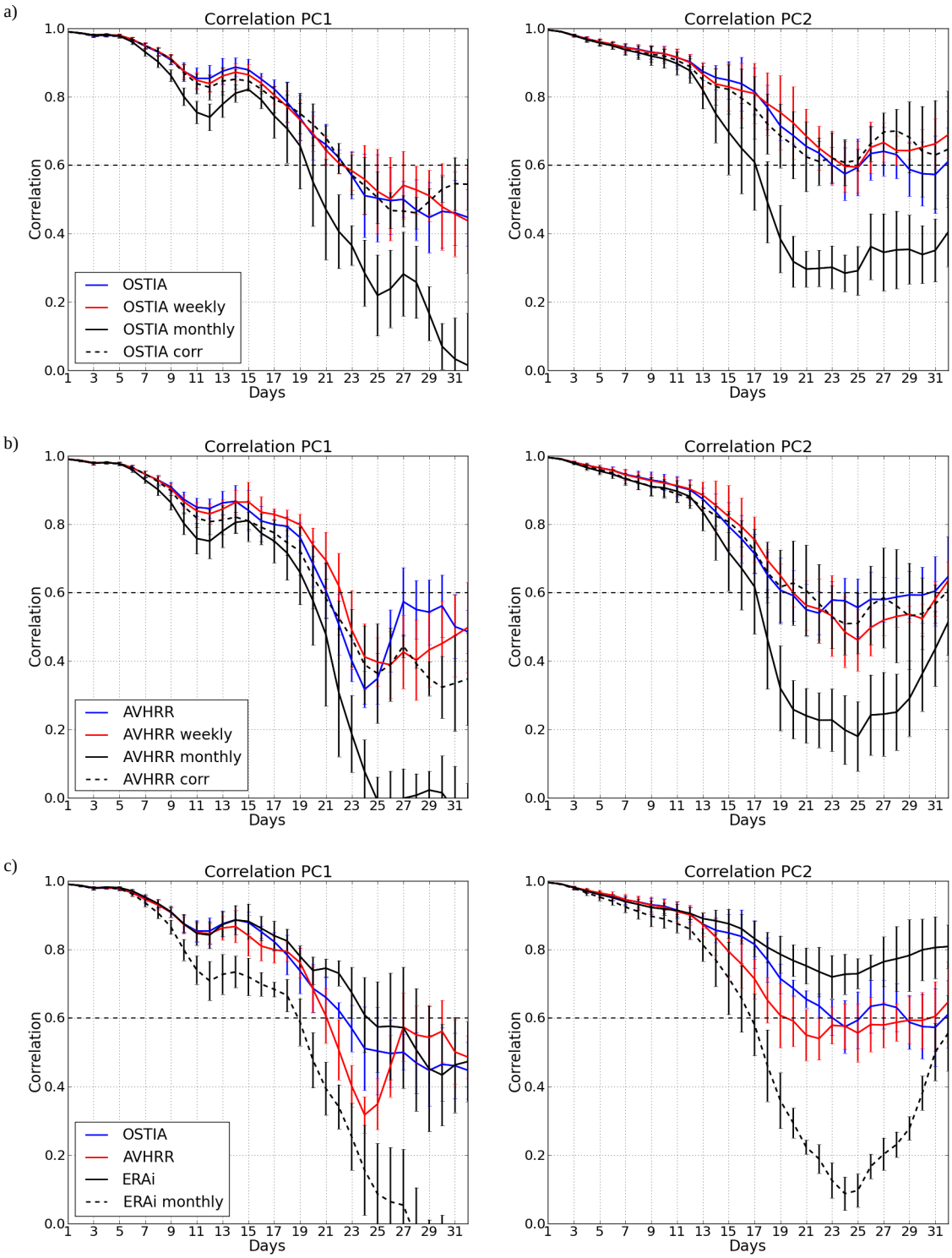

Fig. 5. Correlation of the PC1 (left) and PC2 (right) from the reanalysis with the ensemble mean forecast time series, based on 47 start dates (15 December 1992 to 31 January 1993), for the atmosphere-only experiments performed with the ECMWF forecast system at the T_L159 resolution. a) Forcing by OSTIA SST at original (daily) temporal resolution (black line), weekly (blue line) and monthly (red line) temporal resolutions. The black dashed line is the forcing where OSTIA SST mean state is corrected with respect to ERAi SST. b) Same as a) for AVHRR SST. c) Forcing by original OSTIA (blue line) and AVHRR (red lines) products and by ERAi SST at their original (weekly) and monthly resolutions (solid and dashed black lines, respectively). The signifcance level (correlation of 0.6) is highlighted by a horizontal black dashed line. Error bars stand for the ensemble spread.

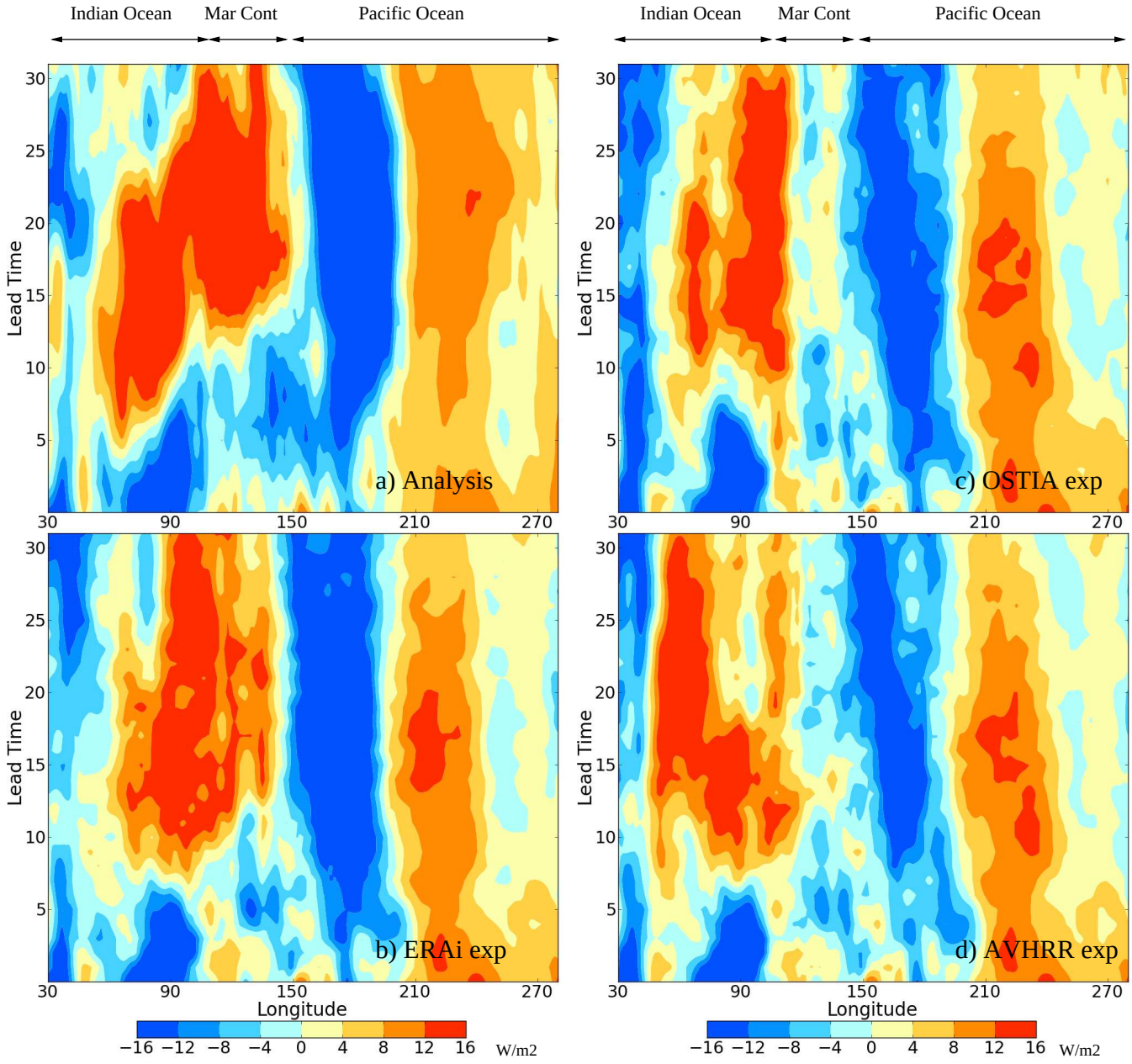

Fig. 6. Longitudinal hovmoller diagrams of the ensemble-mean OLR anomalies (in $W.m^{-2}$) averaged between 10°S and 10°N) for starting dates when the convective centre of the MJO is over the Indian Ocean. Negative anomalies indicates active convection while positive anomalies indicates suppressed convection. a) ERA interim analysis, b) ERAi experiment, c) OSTIA experiment.

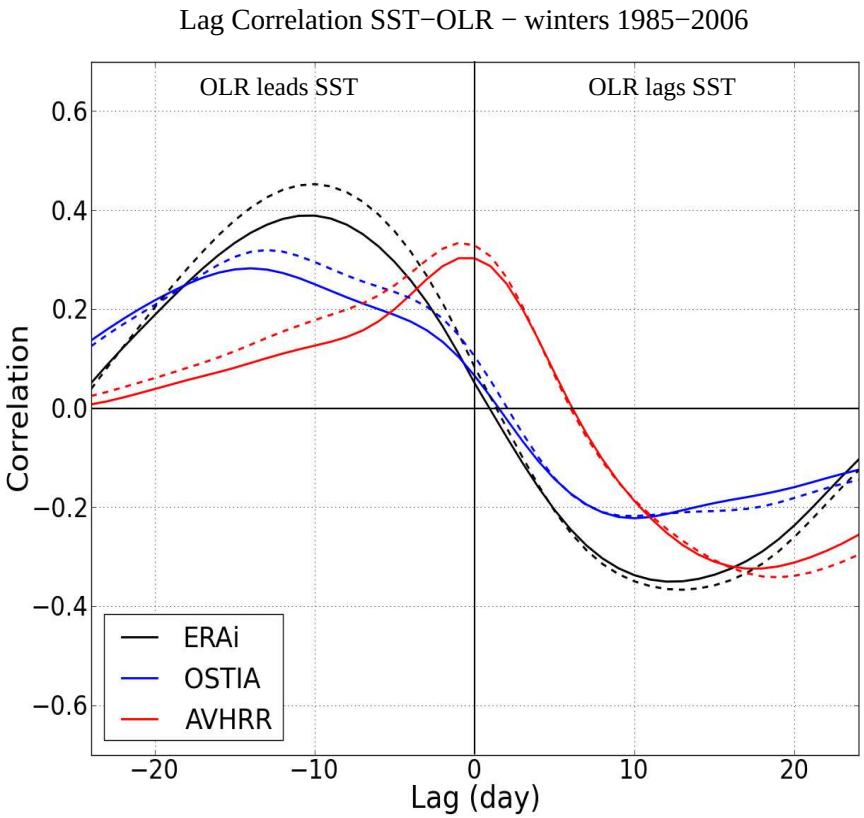

Fig. 7. Lag correlation coefficient between OLR and SST anomalies over the region 5°S-5°N,60°-95°E over the winters (December-February) 1985-2006 using SST fields from ERA interim (ERAi, black lines), OSTIA (blue lines) and AVHRR (red lines) and OLR fields from either ERA interim (solid lines) or NOAA satellites (dashes lines). The lags are in days. OLR leads SST for negative lags and OLR lags SST for positive lags.

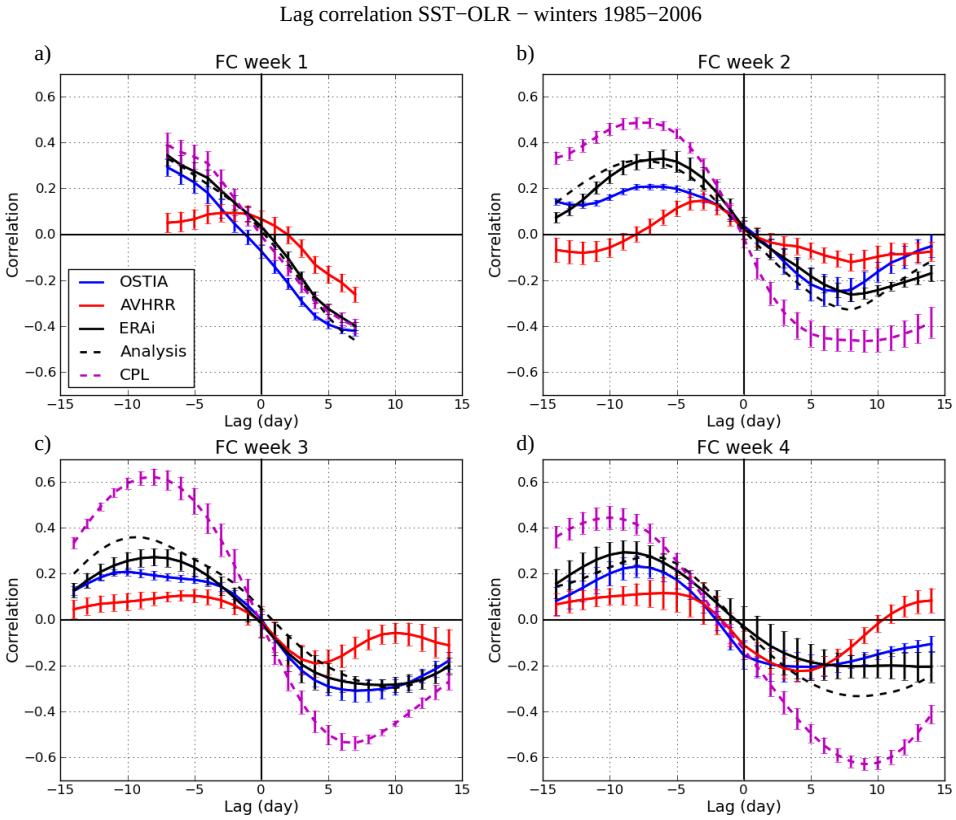

Fig. 8. Lag correlation coefficient between OLR and SST anomalies over the region 5°S-5°N,60°-95°E averaged according to the forecast week of the experiments conducted over 22 winters (1985-2006). OSTIA, AVHRR and ERAi experiments are the blue, red and solid black lines, respectively. Their equivalent in the ERA interim reanalysis is the black dashed line. For comparative purposes, the coupled experiment is plotted in dashed purple. a) Week 1, b) 2, c) 3 and d) 4. Error bars stand for the ensemble spread.

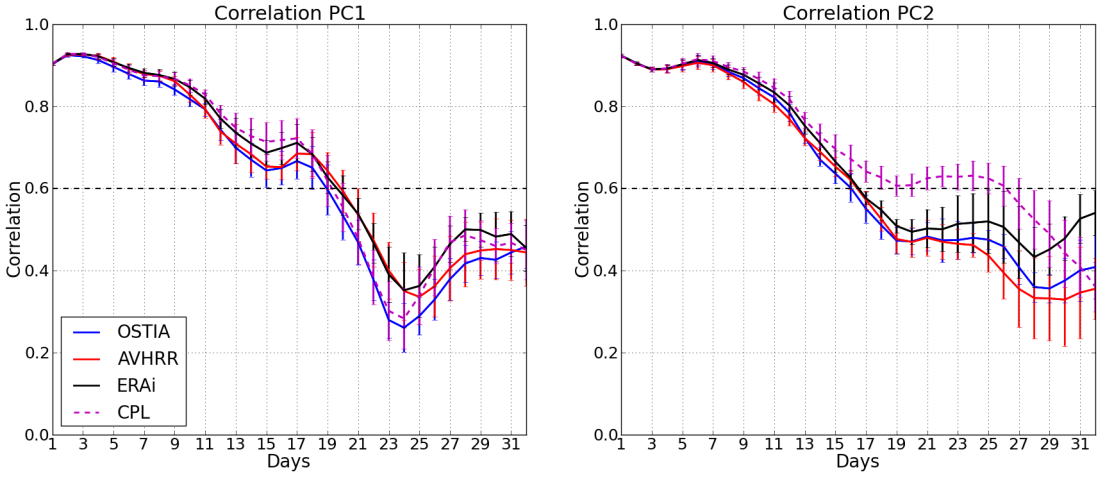

Fig. 9. Same as Fig5 for the experiments conducted over 22 winters from 1985 to 2006: OSTIA, AVHRR and ERAi experiments are the blue, red and black lines, respectively. For comparative purposes, the coupled experiment is plotted in dashed purple.

Table 1. Experiments performed with the ECMWF model in atmosphere-only mode and their respective SST forcing for the MJO case of the winter 1992-1993.

	ERAi SST	**OSTIA SST**	**AVHRR SST**
1	original ERAi	original OSTIA	original AVHRR
2		weekly OSTIA	weekly AVHRR
3	monthly ERAi	monthly OSTIA	monthly AVHRR
4		Corr. mean state	Corr. mean state